Locating Schumann Resonant Frequencies on a Single Particle Radiation Patterns Using Golden Ratio Spiral

Mert Yücemöz

[1]University of Bath

Key Points:

- Located total of two Schumann resonant frequencies in the outer parts of the Dipole and Distorted Dipole radiation patterns.
- Located total of six Schumann resonant frequencies in the centre of the Forward-Backward radiation pattern.
- Relativistic particles radiate three-four times more Schumann resonant frequencies than non-relativistic particles.

Corresponding author: Mert Yucemoz, m.yucemoz@bath.ac.uk

Abstract

Although lightning discharge is not the only source or only physical phenomenon that affects the Schumann resonances, they have the highest contribution to the Schumann resonances oscillating between the ground the ionosphere. Schumann resonances are predicted through several different numerical models such as the transmission-line matrix model or partially uniform knee model. Here we report a different prediction method for Schumann resonances derived from the first principle fundamental physics combining both particle radiation patterns and the mathematical concept of the Golden ratio. This prediction allows the physical understanding of where Schumann resonances originate from radiation emitted by a particle that involves many frequencies that are not related to Schumann resonances. In addition, this method allows to predict the wave propagation direction of each frequency value in the Schumann frequency spectrum. Particles accelerated by lightning leader tip electric fields are capable of contributing most of the Schumann resonances. The radiation pattern of a single particle consists of many frequencies that there are only specific ones within this pattern that contribute to the Schumann radiation. Vast majority of Schumann resonances distribute quite nicely obeying the Golden ratio interval. This property used in conjunction with the full single-particle radiation patterns also revealed that high-frequency forward-backward peaking radiation patterns as well as low-frequency radiation patterns can contribute to Schumann resonances. Moreover, this also allows to locate them on the full radiation pattern. Furthermore, theoretical analysis using Golden ratio spiral predicts that there are more Schumann resonances in high frequency forward-backward peaking radiation pattern of relativistic particle than low frequency dipole radiation pattern.

Plain Language Summary

Particles emit radiation in different shapes. These radiation shapes consist of many different frequencies. However, certain frequencies are capable of oscillating between the ionosphere and the ground and these are called Schumann Resonances which is discovered by German physicist Winfried Otto Schumann. These Schumann frequencies distinguish from each other with the multiples of a special number 1.618 which is called the Golden ratio. By using this property of Schumann resonances, every Schumann frequency can be located on every single particle's radiation pattern. This enables to predict which of the many Schumann resonances would dominate as well as their wave propagation direction.

1 Introduction

Most of the Schumann resonances are generated by lightning discharges. They travel around the world between the ground and the ionosphere. Schumann resonances first predicted by the Schumann (Schumann, 01 Feb. 1952) and detected and experimentally proven to be associated by lightning discharges in 1960 (Balser & Wagner, 1960). This information is also used to work backward and determine lightning activity by measuring the variations in Schumann Resonance in the ionosphere ("Long-term periodical variations in global lightning activity deduced from the Schumann resonance monitoring", 1999). Schumann Resonances detected between the ground, and the ionosphere ranges from 5 to 30 Hz (Heckman et al., 1998). Schumann resonances vary as a result of lightning discharges and cosmic particles (Protons) coming from Solar flares. These Schumann variations were measured by YS station in China, and their horizontal magnetic field component was found to vary and increase by 0.1 to 0.2 Hz. Whereas, vertical magnetic field component decreases by $\sim$ 0.6 Hz (Zhou & Qiao, 2015). In addition, lower frequency within the Schumann resonance spectrum is sensitive and subject to variations mainly due to as a result of observation distance from the source (Ondrášková et al., 2007). Schumann resonances are predicted with numerical methods such as the partially uniform knee model

(Pechony & Price, 2004) or with the Transmission Line Matrix model (Morente et al., 2003). When the peak values in a simulated spectrum of Schumann resonance are analyzed, vast majority of the peaks that represent Schumann resonances are scaled with the Golden ratio (Price, 2016, p.4 , Figure 2). In addition, this is also true with the vast majority of Schumann resonance measurements (Price, 2016, p. 5 , Figure 4). This paper introduces a novel method in locating Schumann resonances on different radiation patterns of a single particle. When used, for instance, with Monte Carlo simulation, it could help understand the generation and variations in magnitudes of the frequencies of the Schumann resonances that are observed by experiments. This enables to predict the most dominant and frequent of Schumann resonances out of many.

2 Theory of Golden Ratio Schumann Resonances Locations on a Radiation Pattern

The Golden ratio is a ratio that can be found to apply to many geometries in nature, maths, and the music. For instance, dividing two consecutive numbers in a Fibonacci sequence always results in a Golden ratio which has a value of $\sim$1.618. In addition, spiral arms of the Milky Way galaxy, or snail shells.

Knowing that most of the Schumann resonant frequencies scale with the Golden ratio has an important application that allows them to be located on a radiation pattern. Not all frequency ranges in a single radiation pattern can oscillate between the ground and the ionosphere. Therefore, by locating these Schumann resonant frequencies in a single radiation pattern, and transforming this single-particle Schumann resonance information to a multiple particle Schumann resonance with a Monte Carlo simulation, the overall magnitude, and frequency range of Schumann resonance can be predicted.

Property of a Golden spiral G_s [m] is that it expands at a Golden ratio and it is given in polar coordinates as

$$G_s = ae^{b\theta_{n,\beta}} \tag{1}$$

Where constant expansion rate "b" $[rad^{-1}]$ of a spiral is Golden ratio given as $b = ln(\frac{1+\sqrt{5}}{2})\frac{2}{\pi}$. In addition, $\theta_{n,\beta}$ [rad] is the Solid angle which gives information about the radiation intensity around an accelerated single particle.

The initial length "a [m]" of a spiral is chosen such that it intersects as many points as possible on a given radiation pattern. Choosing a bigger spiral length than the radiation pattern could lead to missing intersection points between the Golden spiral and the radiation pattern, hence the Schumann resonances.

3 Results

In this section, the Golden spiral given by equation 1 is plotted on the main single particle radiation pattern of Dipole, distorted dipole, and forward-backward peaking. The spiral was set to expand with a Golden ratio from the point zero of origin representing 0 Hz frequency, and to locate Schumann resonances on the radiation pattern of the single-particle which also scales and progresses with Golden ratio. Referred radiation patterns were predicted and presented in the previous publication called "Asymmetric Backward Peaking Radiation Pattern from a Relativistic Particle Accelerated by Lightning Leader Tip Electric Field", (Yucemoz & Füllekrug, 2020).

Afterward, small Golden rectangles are drawn tangent to Golden spiral by moving and expanding section by section in the outward direction. The length of the vertical side to the horizontal side of a Golden rectangle is the Golden ratio. This is same as saying the midpoint of a vertical side to the midpoint of a horizontal side also scales with the Golden ratio. This is true for any correlated identical point on vertical and horizontal sides of the Golden rectangle. All in all, to identify two-point as Schumann resonance, one of the points must be associated with the vertical side of the Golden rectangle, and the other point to the horizontal side. When this requirement is satisfied, two-points are related to each other with a Golden ratio. This property makes them a good candidate for being the Schumann resonances.

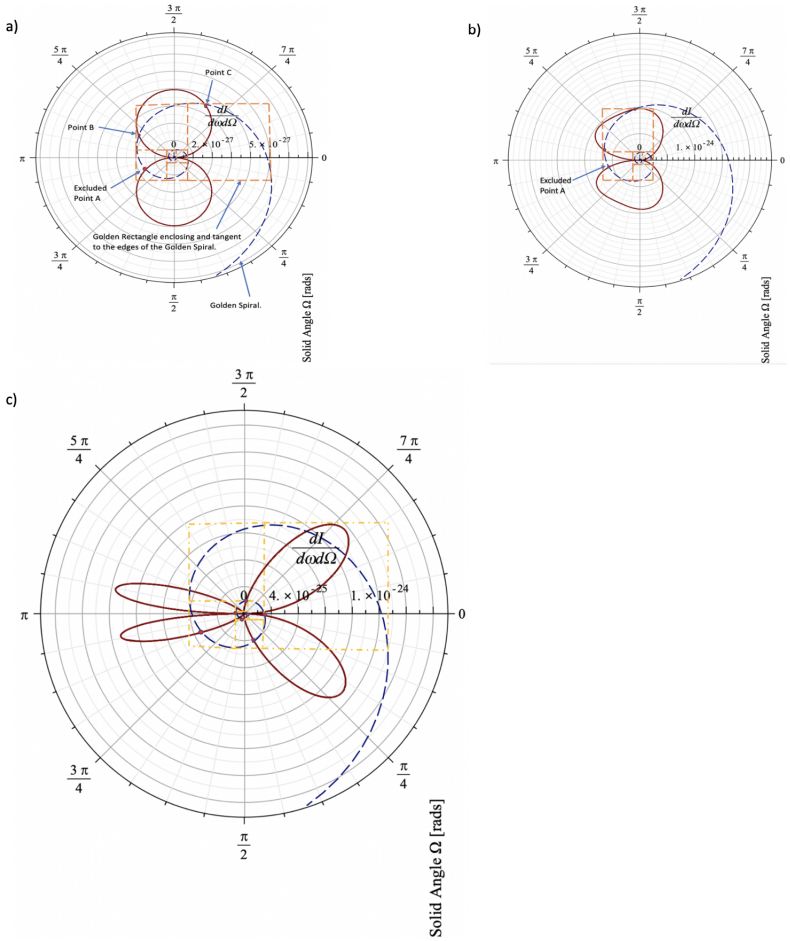

Figure 1. Figure 1 displays three important different types of main radiation patterns where other patterns are just the derivatives from the main radiation patterns. Each point on the graphs is named A, B, C, D... starting from the origin and expanding with the spiral. Like Fibonacci sequences, Schumann resonances distinguishes from each other with the Golden ratio. The Golden spiral expands with a magnitude of Golden ratio. Radiation patterns consists of different frequency ranges. This frequency range widens as the particle becomes relativistic. Therefore, it is important to understand the source of Schumann resonances and locate their position on a radiation pattern. Towards the center of the radiation pattern, radiation frequency decreases. Hence, as the Schumann resonances are low-frequency waves, the Golden spiral has to start from the origin of 0 Hz and progressively expand with a Golden ratio to help locate Schumann resonances. Afterward, Golden rectangle forms tangent around any section of the Golden spiral provided every side of the Golden rectangle is tangent to the Golden spiral. To confirm a point as a Schumann resonance, two points must have a Golden ratio, and the one must occur on the vertical, and the other must occur on the horizontal side of the Golden rectangle. In addition, figure 1a and 1b are low-frequency radiation patterns and have Schumann resonances on the edges. Whereas, figure 1c is a high frequency radiation pattern and have Schumann resonances at the center of the radiation pattern where the frequency is low. All in all, the Golden spiral approach displays a good prediction performance. It does not predict Schumann resonances at the outer parts of the high-frequency radiation pattern 1c, which would contradict with them being Schumann resonance, as Schumann resonance is a low-frequency wave.

Energy values of each Schumann point and their relation to each other in Figure 1a	
Schumann Resonance Point	Radiation radiation intensity "I" $[Js^{-1}]$ per emitted angular wave frequency "ω" $[rads^{-1}]$ per Solid angle "Ω" $[rad]$ $\frac{dI}{d\omega d\Omega}$
A	$\sim 1.456 \times 10^{-27}$
B	$\sim 1.865 \times 10^{-27}$
C	$\sim 3.159 \times 10^{-27}$

Table 1. Values of Schumann points B and C and Golden ratio of C to B in figure 1a.

Energy values of each Schumann point and their relation to each other in Figure 1b.	
Schumann Resonance Point	Radiation radiation intensity "I" $[Js^{-1}]$ per emitted angular wave frequency "ω" $[rads^{-1}]$ per Solid angle "Ω" $[rad]$ $\frac{dI}{d\omega d\Omega}$
A	$\sim 5.428 \times 10^{-25}$
B	$\sim 6.080 \times 10^{-25}$
C	$\sim 9.532 \times 10^{-25}$

Table 2. Values of Schumann points B and C and Golden ratio of C to B in figure 1b.

Energy values of each Schumann point and their relation to each other in Figure 1c.	
Schumann Resonance Point	Radiation radiation intensity "I" $[Js^{-1}]$ per emitted angular wave frequency "ω" $[rads^{-1}]$ per Solid angle "Ω" $[rad]$ $\frac{dI}{d\omega d\Omega}$
A	$\sim 2.15 \times 10^{-26}$
B	$\sim 3.54 \times 10^{-26}$
C	$\sim 5.632 \times 10^{-26}$
D	$\sim 9.483 \times 10^{-26}$
E	$\sim 1.454 \times 10^{-25}$
F	$\sim 2.217 \times 10^{-25}$
G	$\sim 3.390 \times 10^{-25}$

Table 3. Values of Schumann points A, B, C, D, E and F. Golden ratio of B to A, C to B, D to C, F to E and G to F in figure 1c.

As can be seen in Tables 1 and 2 of Figures 1a and 1b, point A is excluded from being a Schumann resonance. Point A does not form a couple with any other point on Golden square vertical and horizontal edges with a Golden ratio.

4 Discussion & Conclusion

As can be seen from figure 1c, the Golden Spiral and Golden rectangle approach haven't predicted any Schumann resonances at the outer parts of the high-frequency forward-backward radiation pattern. All the Schumann resonances for the high-frequency radiation pattern figure 1c was predicted to occur in the center of the forward-backward radiation pattern where the frequency (Directly related with radiation intensity) of the radiated wave is at the minimums. This indicates a good sign that the prediction method is quite reliable as Schumann resonances are low frequency and not high-frequency waves.

Example radiation patterns presented in figure 1c could have different radiation intensities. However, this does not change the predicted locations of the Schumann resonances in figures 1a, 1b, and 1c as these Schumann points rely on the ratio of the radiation intensity values of the two points, which would change accordingly at the same rate to preserve the Golden ratio.

Acknowledgments

I would like to thank my supervisor Dr.Martin Füllekrug for all the support throughout my PhD. My family for their support and good wishes. EPSRC and MetOffice sponsor my PhD project under contract numbers EG-EE1239 and EG-EE1077. The Maple worksheets used to simulate the radiation patterns with the Golden Ratio spiral to locate the Schumann resonances are openly available from the University of Bath Research Data Archive at https://doi.org/10.15125/BATH-00914.

References

Balser, M., & Wagner, C. A. (1960). Observations of earth–ionosphere cavity resonances. *Nature*, *188*(4751), 638–641. Retrieved from https://doi.org/10.1038/188638a0 doi: 10.1038/188638a0

Heckman, S. J., Williams, E., & Boldi, B. (1998). Total global lightning inferred from schumann resonance measurements. *Journal of Geophysical Research: Atmospheres*, *103*(D24), 31775-31779. Retrieved from https://agupubs.onlinelibrary.wiley.com/doi/abs/10.1029/98JD02648 doi: 10.1029/98JD02648

Long-term periodical variations in global lightning activity deduced from the schumann resonance monitoring. (1999). *Journal of Geophysical Research: Atmospheres*, *104*(D22), 27585-27591. Retrieved from https://agupubs.onlinelibrary.wiley.com/doi/abs/10.1029/1999JD900791 doi: 10.1029/1999JD900791

Morente, J. A., Molina-Cuberos, G. J., Portí, J. A., Besser, B. P., Salinas, A., Schwingenschuch, K., & Lichtenegger, H. (2003). A numerical simulation of earth's electromagnetic cavity with the transmission line matrix method: Schumann resonances. *Journal of Geophysical Research: Space Physics*, *108*(A5). Retrieved from https://agupubs.onlinelibrary.wiley.com/doi/abs/10.1029/2002JA009779 doi: 10.1029/2002JA009779

Ondrášková, A., Kostecký, P., Ševčík, S., & Rosenberg, L. (2007). Long-term observations of schumann resonances at modra observatory. *Radio Science*, *42*(2). Retrieved from https://agupubs.onlinelibrary.wiley.com/doi/abs/10.1029/2006RS003478 doi: 10.1029/2006RS003478

Pechony, O., & Price, C. (2004). Schumann resonance parameters calculated with a partially uniform knee model on earth, venus, mars, and titan. *Radio Science*, *39*(5), 1-10.

Price, C. (2016). Elf electromagnetic waves from lightning: The schumann resonances. *Atmosphere*, *7*(9). Retrieved from https://www.mdpi.com/2073-4433/7/9/116 doi: 10.3390/atmos7090116

Schumann, W. O. (01 Feb. 1952). Über die strahlungslosen eigenschwingungen einer leitenden kugel, die von einer luftschicht und einer ionosphärenhülle umgeben ist. *Zeitschrift für Naturforschung A*, *7*(2), 149 - 154. Retrieved from https://www.degruyter.com/view/journals/zna/7/2/article-p149.xml doi: https://doi.org/10.1515/zna-1952-0202

Yucemoz, M., & Füllekrug, M. (2020). Asymmetric backward peaking radiation pattern from a relativistic particle accelerated by lightning leader tip electric field. *Earth and Space Science Open Archive*, 28. Retrieved from https://doi.org/10.1002/essoar.10503599.1 doi: 10.1002/essoar.10503599.1

Zhou, H., & Qiao, X. (2015). Studies of the variations of the first schumann resonance frequency during the solar flare on 7 march 2012. *Journal of Geophysical Research: Atmospheres*, *120*(10), 4600-4612. Retrieved from https://agupubs.onlinelibrary.wiley.com/doi/abs/10.1002/2014JD022696 doi: 10.1002/2014JD022696